Fault Diagnosis of Power Supply Equipment Based on Distributed Fiber Grating Temperature Sensing

Gang Wang*
Beijing Jingneng Clean Energy Co., Limited, Beijing, 100028, China
**Corresponding Author.*

Abstract

Power supply system is the foundation to ensure the orderly operation of various industries, and its fault monitoring and maintenance is one of the most critical tasks. Aiming at the problems of low efficiency and poor real-time performance of manual inspection, a long-distance temperature measurement system based on distributed fiber grating is proposed in this paper. Firstly, the packaging structure of the grating sensing unit is designed to realize the decoupling of temperature-deformation spectral drift. The temperature sensitivity is 10.79pm/℃, and the repeatability is better than ±0.1 ℃. Secondly, an 8-channel distributed fiber grating temperature monitoring system is designed. The sensors are arranged in the switchgear and transformer of the device to realize the all-weather accurate fault monitoring of the power supply system. Since its operation, the system has been working stably and successfully warned of multiple power supply equipment failures. It provides effective technical support for the construction of smart power systems, and has broad application prospects in power supply equipment health monitoring.

Keywords: *fiber grating, temperature sensing, power supply system, fault monitoring*

I. Introduction

Power supply equipment plays an extremely important role in modern industrial and agricultural production and people's daily life. Its troubleshooting and maintenance have always been one of the most critical tasks for power supply guarantee [1-2]. Setting up temperature sensors to monitor power supply equipment all-weather is the main method to overcome the disadvantages of manual inspection [3-4]. Conventional temperature measurement technology is mainly divided into two methods: wired temperature measurement [5-6] and wireless temperature measurement[7-9]. Each measuring point needs to connect the signal line to the signal collector separately. For multi-point layout, the amount of cables is huge, resulting in the risk of overlapping and short circuit between transmission line and power transmission line. There are also disadvantages in electric signal transmission distance and electromagnetic interference. Wireless sensor solves the wiring problem, but the control of wireless signal in special occasions leads to poor practical operability.

Optical fiber sensing technology is a new sensing technology [10-12]. Optical fiber is both a sensor and a signal transmission medium. It is made of natural insulation, has no electromagnetic interference problem and has low transmission loss. It is suitable for long-distance and large-scale regional monitoring applications. In 2000, German Siemens began to study the application of fiber grating sensor in the temperature monitoring of air-cooled turbine generator stator, with a measurement range of 20 ℃-160 ℃ and an accuracy of less than 1 ℃ [13]. Hokkaido, Japan has also reported the use of fiber grating sensors to measure the snow load of high-voltage transmission cables [14]. In 2018, Rodriguez et al. used a fiber grating temperature sensor to measure the temperature change of the three-phase thyristor rectifier bridge in the generator during the start-up phase of the generator [15]. In 2019, Sun et al. used 4 fiber grating temperature sensors to measure the temperature of the transformer, but did not report the engineering application effect [16].

Based on this, this paper proposes a fault monitoring method for long-distance power supply equipment based on

distributed fiber grating temperature sensing. Firstly, the packaging structure of the fiber grating is designed to realize the decoupling of temperature and strain. The temperature sensitivity is tested to be 10.79pm/℃, and the repeatability within 15 minutes is better than ±1pm. The 8-channel fiber grating is encoded by wavelength division multiplexing and arranged in different positions of different power systems to realize all-weather and real-time fault monitoring. The system has accurately warned of many failure cases, providing important technical support for the construction of smart power.

II. Design of Fiber Bragg Grating Temperature Sensor

The reflection wavelength λ of the fiber grating depends on the effective refractive index n_{eff} of the core and the grating period Λ, and the equation is expressed as [17]:

$$\lambda_B = 2n_{eff}\Lambda \tag{1}$$

From Eq. (1), the change of the grating resonance wavelength caused by the effective refractive index or the grating period is:

$$\Delta\lambda_B = 2\left(\Delta n_{eff}\Lambda + n_{eff}\Delta\Lambda\right) \tag{2}$$

The change of grating resonance wavelength with strain and temperature is:

$$\frac{\Delta\lambda_B}{\lambda_B} = \left(1-\rho_z\right)\Delta\varepsilon + \left(\alpha+\beta\right)\Delta T \tag{3}$$

where, Δε, ΔT and ρ_z are the strain change, temperature change and effective elasticity coefficient, respectively. α and β are the thermal expansion coefficient and the thermo-optic coefficient, respectively. Since the fiber grating temperature sensor only responds to temperature, it is necessary to package the grating to make it insensitive to the deformation of the object to be measured.

In this paper, a C-shaped metal material and ceramic sheet are combined to isolate the strain. The schematic diagram of the package is shown in Fig. 1. In order to ensure the response speed of the sensor, the substrate is made of metal with extremely fast thermal conductivity. At the same time, in order to prevent the substrate strain from being directly transmitted to the fiber grating, a ceramic sheet is used to isolate the strain. The gate area is suspended, and the two ends are fixed to the ceramic substrate. As a part of the arc, the fixed points at both ends of the fiber Bragg grating are A and B, respectively. L is the arc length; r is the arc radius, y is the standard chord length corresponding to the arc, and x is the distance from the top of the arc to the chord.

$$r = \frac{x^2 + (\frac{y}{2})^2}{2x} \quad \text{and} \quad \theta = \tan(\frac{xy}{(y/2)^2 - x^2}) \tag{4}$$

Assuming that the ceramic substrate y has a strain Δy, the change in the distance x between the grid area and the ceramic base is Δx, then the change in arc length L=2θr is

$$\Delta L = \frac{(x+\Delta x)^2+(y/2)^2}{x} \times \tan\left(\frac{x(y+\Delta y)}{\left(\frac{y+\Delta y}{2}\right)^2-(x+\Delta x)^2}\right) - \frac{x^2+(y/2)^2}{x} \times \tan\left(\frac{xy}{(y/2)^2-x^2}\right) \tag{5}$$

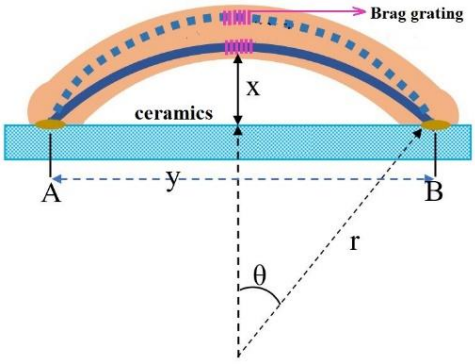

Fig.1Schematic diagram of C-shaped strain decoupling temperature sensor

According to the strain decoupling principle, the strain variable can be expressed as:

$$\varepsilon = \frac{\Delta L - (\Delta L_1 - y)}{L_1} \tag{6}$$

If $\Delta L \leq L_{1-y}$, there will be strain decoupling effect. If $\Delta L > L_{1-y}$, there is no decoupling effect.

COMSOL software is used to perform finite element analysis on the structure [17-18], and simulation is fulfilled according to the real size of the sensor (y=30mm, x=2mm). Since the sensor is installed on the power supply device, when performing finite element simulation analysis on the sensor, the bottom of the sensor base is first fixed on the aluminum plate, and then the grid is divided. After that, the stretched part, the sensor housing, the ceramic sheet and the fiber grating are cut, combined and swept to mesh. One end of the tensile member is fixed and a tensile force of 660 με at the other end is applied. The force cloud diagram of each component is obtained by simulation as shown in Fig. 2.

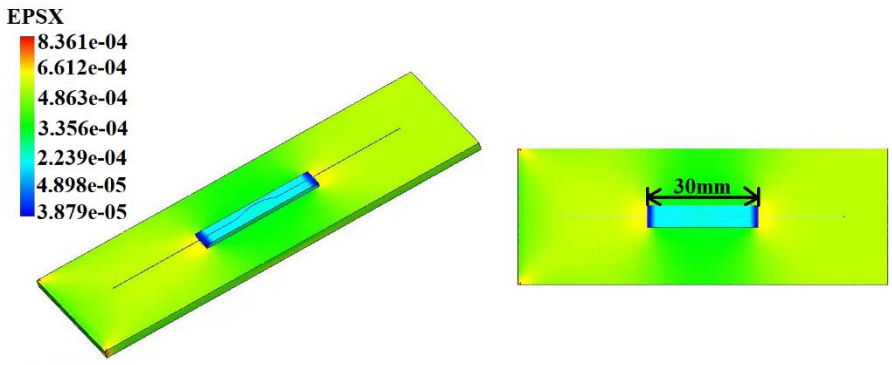

Fig.2 Stress diagrams of tensile parts, substrates, ceramic sheet and fiber gratings

Fig. 2 are the force cloud diagrams of the substrate, ceramic sheet and fiber grating, respectively. It can be seen that in the case of stretching 660 με, the strain of the ceramic sheet is less than 388 με, and the fiber grating is in a force-isolated state. At the same time, through the C-shaped bending of the fiber grating, a stretch buffer is reserved to ensure that in the deformation range of the power supply system, the interference error caused by the strain on the temperature measurement can be effectively eliminated.

III. Temperature sensor performance test

In order to obtain the performance parameters of the designed temperature sensor, five fiber grating temperature

sensors with center frequencies of 1532nm(FBG1), 1534nm(FBG2), 1536nm (FBG3), 1542nm (FBG4), 1544nm (FBG5)are placed in a high-precision constant temperature water bath (fluke company, accuracy 0.01 °C). The test system is shown in Fig.3. FBG1-FBG5 are five sensors with different central wavelengths that are fused on the same optical fiber.The light of the broad-spectrum light source ASE is input into the optical fiber and path through the wavelength division multiplexer WDM. The reflection spectra of different gratings are read out from the spectrometer.The temperature adjustment range is 10 ℃-40 ℃; the temperature change interval is 10 ℃, and the temperature stabilization time of each test is 15min.

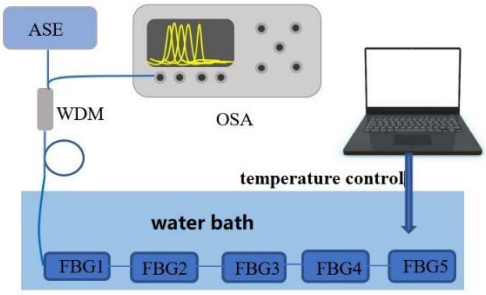

Fig. 3 Schematic of temperature calibration system

The temperature adjustment range is 10 ℃-40 ℃, and the change interval is 10 ℃. The stability time of each test temperature is 15min to obtain the wavelength drift of the sensor in the whole process. Fig. 4(a) shows the variation of the wavelength of FBG5 with the temperature of water bath. The experiment is repeated five times, and the wavelength of each time at constant temperature is averaged. The repeatability of five experiments FBG5 is obtained. As shown in Fig. 4 (b), the maximum wavelength drift at each temperature is ± 2pm. Table 1 is the repeatability of the five sensors at different temperatures.

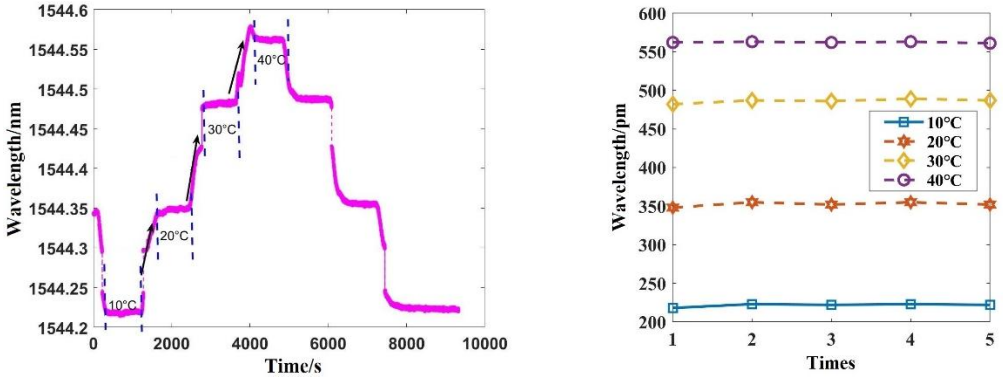

(a) (b)

Fig. 4 Temperature calibration process and repeatability

Table 1. 15-minute repeatability of five sensors at different temperatures

	FBG1	FBG2	FBG3	FBG4	FBG5
10 ℃	±1pm	±1pm	±1pm	±1pm	±0.5pm
20 ℃	±0.5pm	0	±0.5pm	±0.5pm	±1pm
30 ℃	±1pm	±0.5pm	0	±1pm	±0.5pm

40 ℃	±0.5pm	±1pm	±1pm	±1pm	±1pm

The center wavelength values collected by each sensor at different temperatures are respectively subjected to first-order linear fitting, and the results are shown in Fig. 5.The temperature sensitivity coefficients are 110.79pm/ ℃, 10.85pm/ ℃, 12.01pm/ ℃, 11.75pm/ ℃ and 11.66pm/ ℃ respectively, and the average linearity is better than 99.29%.

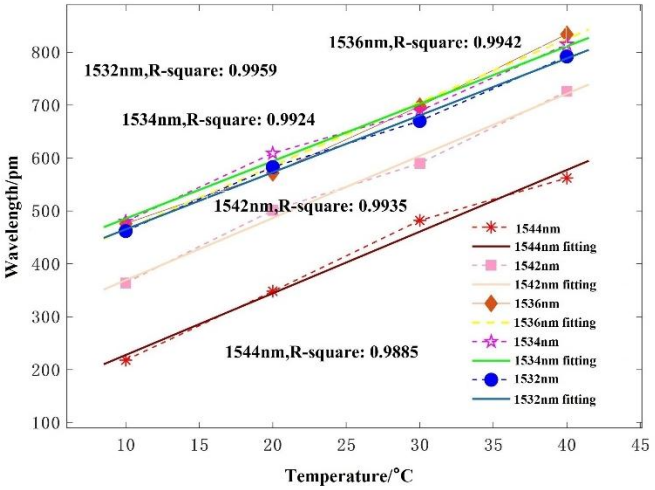

Fig. 5 Calibration of temperature coefficient of sensor

Generally, according to the maximum repeatability deviation (±1pm) and temperature sensitivity (10.79pm/ ℃) of the temperature sensor, the repeat ability error of this temperature sensor does not exceed ±0.1 ℃.

IV. Temperature fault monitoring of power supply system

According to the monitoring requirements of the power supply system, a long-distance, multi-point distributed fiber grating temperature sensing system is designed in this paper. The system includes three modules: field sensor layout, fiber grating demodulation, and intelligent display terminal. The overall schematic diagram is shown in Fig. 6. The broadband light source is transmitted to the on-site fiber grating sensor through the fiber coupler, and the reflection spectrum is returned by the fiber coupler and received by the CCD module. Through the acquisition and peak seeking of spectral data, the real-time temperature is demodulated and displayed by the intelligent terminal.

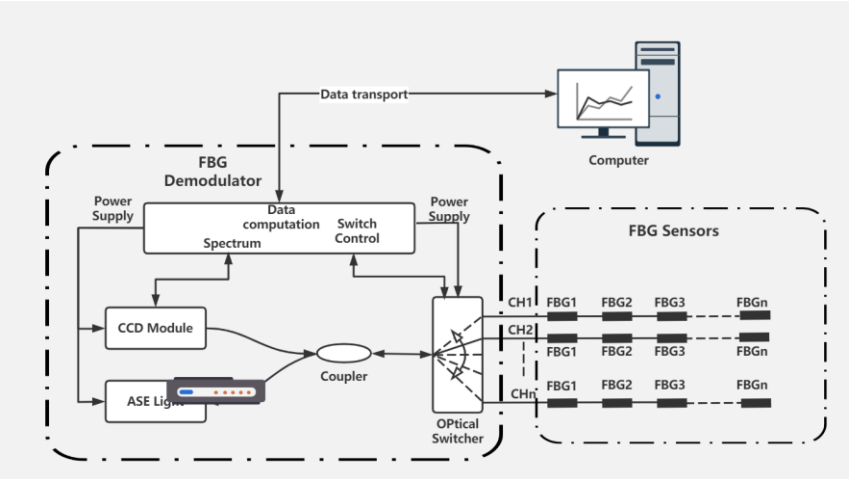

Fig.6 Temperature sensor layout area

A round robin module is set in the demodulation module to collect the spectral data of 8-channel in turn in the way of optical time division multiplexing, and the switching rate is 8Hz to ensure the real-time performance of temperature monitoring. The temperature status of different areas obtained by the whole temperature monitoring system is shown in Table 2.

Table 2 Temperature status in different test areas

Area	Average temperature (℃)	The highest temperature (℃)	The ambient temperature (℃)
Switch cabinet	43.5	44	40
Busbar	38.7	40	32
Transformer	44	44	42

As shown in Fig.7, it is the temperature curve collected when the power supply equipment fails in September 2019. At the beginning of the first 14000 minites, the trend of sensors 1 to 5 is the same. After that, the temperature of sensor 1 is begin to deviate from the trend of the other sensors. When the temperature of sensor is 5℃ higher than that of adjacent measuring points, and the temperature monitoring was diagnosed as a failure of the power supply system. After the overhaul, the temperature measurement results are shown on the 28th and later in the figure. The temperature of the measuring point is consistent with the temperature trend of the adjacent measuring point, which avoids the damage to the equipment caused by the over-temperature load.

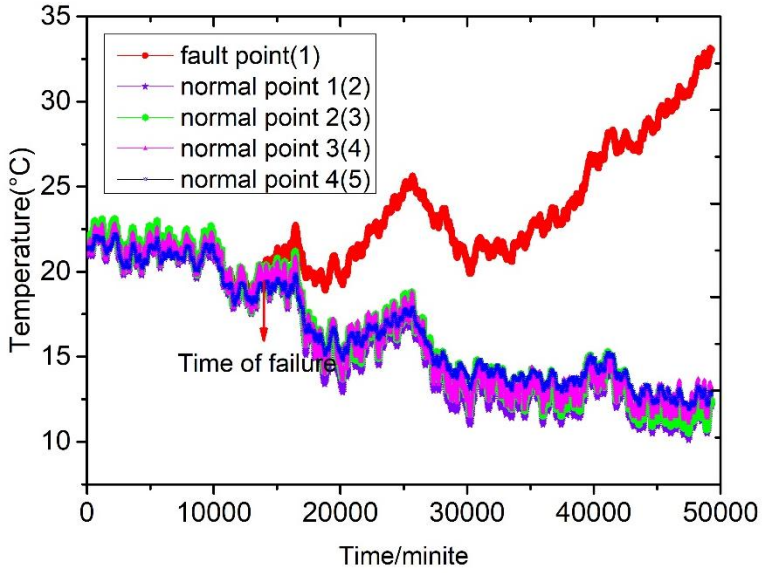

Fig.7 Power supply system failure

V. Conclusion

The C-type packaged fiber grating sensor is designed and calibrated in this paper. On this basis, a long-distance distributed fiber grating temperature sensing system with 8 channels and 23 units per channel is developed for the power supply system for all-weather and long-term temperature monitoring. The system has replaced the current manual inspection method, and greatly improved the accuracy and real-time performance of fault monitoring. It also provides technical support for the safe and orderly operation of the power system, and has broad application prospects in power supply system health monitoring.

References

[1] Kim E, Lee J, Liang H, et al. Offline Guarantee and Online Management of Power Demand and Supply in Cyber-Physical Systems// 2016 IEEE Real-Time Systems Symposium (RTSS). IEEE, 2017.
[2] Dong J, Jin F, Lv H R, et al. Method for detecting conflicts between outage requests and power supply guarantee requests in a power grid. US, 2013.
[3] Yue-Feng L U, Shen Y, Zhao G X, et al. Construction of Power Supply Guarantee Model for Major Events. Construction & Design for Engineering, 2019.
[4] Jin T F. Design of Power Supply Reliability Guarantee System for Mine Local Fan. Mechanical & Electrical Engineering Technology, 2019.
[5] Kuchta R, Vrba R. Wireless and Wired Temperature Data System// International Conference on Systems. IEEE Computer Society, 2007.
[6] Miki Y, Ohwaki Y. Flexible wired circuit board for temperature measurement. US, 2009.
[7] Xiao C. Temperature and Humidity Measurement Based on Wireless Sensor Network Technology. Key Engineering Materials, 2010, 439-440(pt.1):46-50.
[8] Reindl L M, Shrena I M. Wireless measurement of temperature using surface acoustic waves sensors. IEEE Transactions on Ultrasonics Ferroelectrics & Frequency Control, 2004, 51(11):1457.
[9] Huo W J, Yao X H, Fu J Z. A Wireless Temperature Measuring System for Rotating Spindle Based on ZigBee. Advanced Materials Research, 2011, 305:325-329.
[10] Yan Z, Jin S J, Qu Z G. Study on the distributed optical fiber sensing technology for pipeline leakage protection. International Society for Optics and Photonics, 2006.
[11] Rogers A J. Distributed optical fiber sensing. Proceedings of SPIE - The International Society for Optical Engineering, 1991, 1504(8).
[12] Rogers A J, Handerek V A. Frequency-derived distributed optical-fiber sensing: Rayleigh backscatter analysis. Applied Optics, 1992, 31(21):4091-4095.
[13] N.M. Theune, et al. Applications of Fiber Optical Sensors in Power Generations: Current and Temperature Sensors. Proc. of Opto. 2000 Conf. 2000:22-25
[14] Y.Ogawa. et al. A multiplexing load monitoring system for power transmission lines using fiber Bragg grating. Proc. of the Optical Fiber Sensors Conf. Williamsburg, VA, USA, 1997: 468-471
[15] António Barrias, Rodriguez G , Casas J R , et al. Application of distributed optical fiber sensors for the health monitoring of two real structures in Barcelona. Structure & Infrastructure Engineering, 2018.
[16] Sun Yecheng. Research on Multi-parameter Online Monitoring Technology of Transformer Based on Fiber Bragg Grating Sensor. Qilu University of Technology.2019
[17] Long C, White R E. Mathematical modeling of a lithium ion battery with thermal effects in COMSOL Inc. Multiphysics (MP) software. Journal of Power Sources, 2011, 196(14):5985-5989.
[18] Germann P, Menshykau D, Tanaka S, et al. Simulating Organogenesis in COMSOL. 2012.